

# Temperature Dependence of the FIR Reflectance of LaSrGaO<sub>4</sub>

A.W. McConnell<sup>1</sup> and T. Timusk

*Department of Physics and Astronomy, McMaster University, Hamilton, Ontario, Canada L8S 4M1*

A. Dabkowski and H.A. Dabkowska

*Brockhouse Institute of Materials Research, McMaster University, Hamilton, Ontario, Canada L8S 4M1*

## Abstract

The reflectance of single crystal LaSrGaO<sub>4</sub> has been measured from  $\approx 50$  to  $40000\text{ cm}^{-1}$  along the *a* and *c* axis. The optical properties have been calculated from a Kramers-Kronig analysis of the reflectance for both polarization. The reflectance curves have been fit using a product of Lorentzian oscillators.

PACS numbers:78.30 -j

*Key words:* LaSrGaO<sub>4</sub>, thin film substrate, optical reflectivity, far-infrared spectra, phonon spectrum.

## Introduction

The importance of film growth in the field of high temperature HTSC superconductors has lead to a search for new substrates with properties optimized for various applications. The substrates have to be compatible with the film both in physical properties such as lattice parameter, thermal expansion coefficient as well as chemical properties, for example the avoidance of certain elements such as silicon which can diffuse from the substrate to the film. The use of the film in passive microwave devices, or to fabricate Josephson

---

<sup>1</sup> Present address: Department Of Physics, Simon Fraser University, Burnaby, B.C., Canada V5A 1S6.

junctions further restrict the choice of substrate materials. Popular substrate materials for HTSC films include LaAlO<sub>3</sub>, SrTiO<sub>3</sub>, NdGaO<sub>3</sub>, MgO, with the majority of the work being done on YBa<sub>2</sub>Cu<sub>3</sub>O<sub>7- $\delta$</sub> . Recently several groups have begun using the crystal substrate, LaSrGaO<sub>4</sub>, which has some promising properties for the production of microwave devices and Josephson junctions.

LaSrGaO<sub>4</sub> has a tetragonal K<sub>2</sub>NiF<sub>4</sub> structure with the La and Sr distributed statistically on the K sites.[1] The space group of this structure is I4/mmm (D<sub>4h</sub><sup>17</sup>). Seven infrared active modes are predicted by group theory[2]; four E<sub>u</sub> modes perpendicular to the c axis and three A<sub>2u</sub> modes parallel to the c axis.[3] The lattice parameters of LaSrGaO<sub>4</sub> are  $a = 3.84 \text{ \AA}$  and  $c = 12.86 \text{ \AA}$  at room temperature with the  $a$  axis being a close match to the  $a$  and  $b$ -axes of YBa<sub>2</sub>Cu<sub>3</sub>O<sub>7- $\delta$</sub> . The room temperature dielectric constant at 10 GHz is  $\epsilon_1 = 22$  which compares favorably with that of LaAlO<sub>3</sub>. The thermal expansion coefficient along the  $a$  axis is 10 ppm/°C providing a reasonable match to that of YBa<sub>2</sub>Cu<sub>3</sub>O<sub>7- $\delta$</sub>  (12.6 ppm/°C).

Hontsu *et al.* and others have shown that LaSrGaO<sub>4</sub> can be used to grow good quality YBa<sub>2</sub>Cu<sub>3</sub>O<sub>7- $\delta$</sub>  thin films.[4,5] A recent comparison study indicates that the YBa<sub>2</sub>Cu<sub>3</sub>O<sub>7- $\delta$</sub>  films grown on LaSrGaO<sub>4</sub> were of comparable quality in transition temperature, critical current, and surface morphology, to the films grown on LaAlO<sub>3</sub>.[6] Most importantly for microwave applications, LaSrGaO<sub>4</sub> does not suffer from any phase transition which can lead to twinning as does LaAlO<sub>3</sub>. It has been reported that LaSrGaO<sub>4</sub> has been used to produce YBa<sub>2</sub>Cu<sub>3</sub>O<sub>7- $\delta$</sub>   $a$  axis films which display a high degree of in-plane alignment of the c axis.[7–10] This is of interest because good quality  $a$  axis films may be used in the manufacture of Josephson junctions; they are also convenient for studies of the properties of YBa<sub>2</sub>Cu<sub>3</sub>O<sub>7- $\delta$</sub>  thin films. LaSrGaO<sub>4</sub> has also been used for the growth of  $a$  axis aligned Bi<sub>2</sub>Sr<sub>2</sub>CuO<sub>x</sub> films.[11] A number of studies of junctions utilizing LaSrGaO<sub>4</sub> as a substrate or as a barrier layer have been published, pointing to its potential in device manufacturing.[12–15] One study of a variety of substrates suggests that LaSrGaO<sub>4</sub> may allow the manufacture of a microwave resonator and filter with a temperature independent center frequency.[16]

A study of the infrared properties of the substrate material serves several goals. One can form an estimate of the fundamental microwave properties of a dielectric material from an extrapolation of the low frequency portion of its infrared spectrum.[17] Also, for fundamental studies of the properties of thin films it is often found that if the films are thinner than the microwave penetration depth the fields penetrate into the substrate and the measurements have to be corrected for substrate effects by including corrections that assume a knowledge of the optical constants of the substrate.

Reflectance measurements polarized along the axes of thin films are of use

in comparing the results with those of single crystals and offer a ready technique for characterization when single crystals of sufficient size are difficult to produce. However, a knowledge of the optical properties of the underlying substrate is critical to the interpretation of the spectrum since it is a convolution of the optical properties of both the film and the substrate. With this as a motivation, the optical properties of LaSrGaO<sub>4</sub> were measured along both *a* and *c* polarizations from 50 cm<sup>-1</sup> to 40000 cm<sup>-1</sup>.

## Experimental

The LaSrGaO<sub>4</sub> crystals used were grown at the Brockhouse Institute of Materials Research at McMaster University using a Czochralski growth technique described elsewhere.[18] The samples used for optical measurements were cut in two orientations, (001) for *a* axis measurements and (010) for *c* axis. The samples were polished to an optically smooth finish and mounted on flat holders.

The far infrared (FIR) measurements were made on a Michelson interferometer using an *in situ* gold coating technique to determine the absolute reflectance.[19] We estimate the uncertainty of  $\pm 1\%$  in the overall reflectance level. Bolometer detectors at 1.4K and a 4.2K were used in the 50 cm<sup>-1</sup> to 800 cm<sup>-1</sup> frequency range, and an MCT detector was used from 700 cm<sup>-1</sup> to 7000 cm<sup>-1</sup>. The resolution was 4 cm<sup>-1</sup> up to 800 cm<sup>-1</sup> and 10 cm<sup>-1</sup> between 1000 cm<sup>-1</sup> to 7000 cm<sup>-1</sup>. The samples were cooled by a controlled liquid helium flow through a cold finger.

The remaining frequencies from 7000 cm<sup>-1</sup> to 40000 cm<sup>-1</sup> were measured using a diffraction grating spectrometer using *in situ* deposition of gold or aluminum. The resolution for this region was 200 cm<sup>-1</sup>. The measurements above 800 cm<sup>-1</sup> were made at room temperature, since the samples displayed no significant temperature dependence in the reflectance above this frequency.

## Results

Figure 1 shows the reflectance polarized along the *a* axis from 50 to 1500 cm<sup>-1</sup> at 300 K, 150 K, and 10 K. The inset shows the 300 K *a* axis reflectance for the full range measured, 50 to 40000 cm<sup>-1</sup>. Figure 2 shows the reflectance polarized along the *c* axis from 50 to 1500 cm<sup>-1</sup> for temperatures 300 K, 200 K, 100 K and 10 K. The inset shows the 300 K *c* axis reflectance from 50 to 40000 cm<sup>-1</sup>. The heights of the reflectance peaks can be seen to be increasing with decreasing temperature in a monotonic fashion.

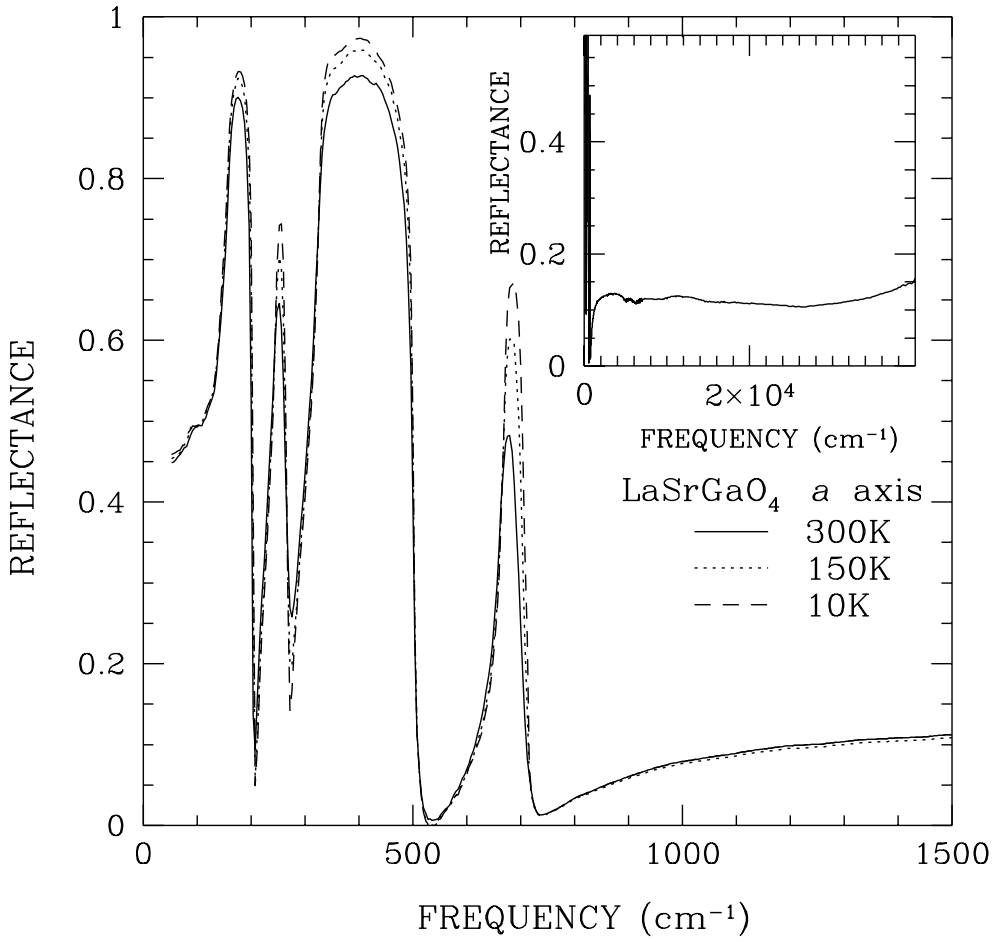


Fig. 1. Temperature dependence of the  $a$  axis reflectance of  $\text{LaSrGaO}_4$  from  $50 \text{ cm}^{-1}$  to  $1000 \text{ cm}^{-1}$  at 300K (solid lines), 150K (dotted line) and 10K (dashed line). The inset shows reflectance spectrum for 300K out to  $40000 \text{ cm}^{-1}$ .

The optical properties of the sample can be extracted from the spectra using Kramers-Kronig transformations to calculate the phase,  $\phi$ , of the reflectivity,  $\tilde{r} = \sqrt{R}e^{i\phi}$ . The optical constants  $\epsilon_1$  and  $\sigma_1$  are then calculated for each frequency using the following equations :

$$n = \frac{1 - R}{1 + R - 2\sqrt{R}\cos(\phi)} \quad (1)$$

$$k = \frac{-2\sqrt{R}\sin(\phi)}{1 + R - 2\sqrt{R}\cos(\phi)} \quad (2)$$

$$\tilde{\epsilon} = \epsilon_1 + i\frac{4\pi\sigma_1}{\omega} \quad (3)$$

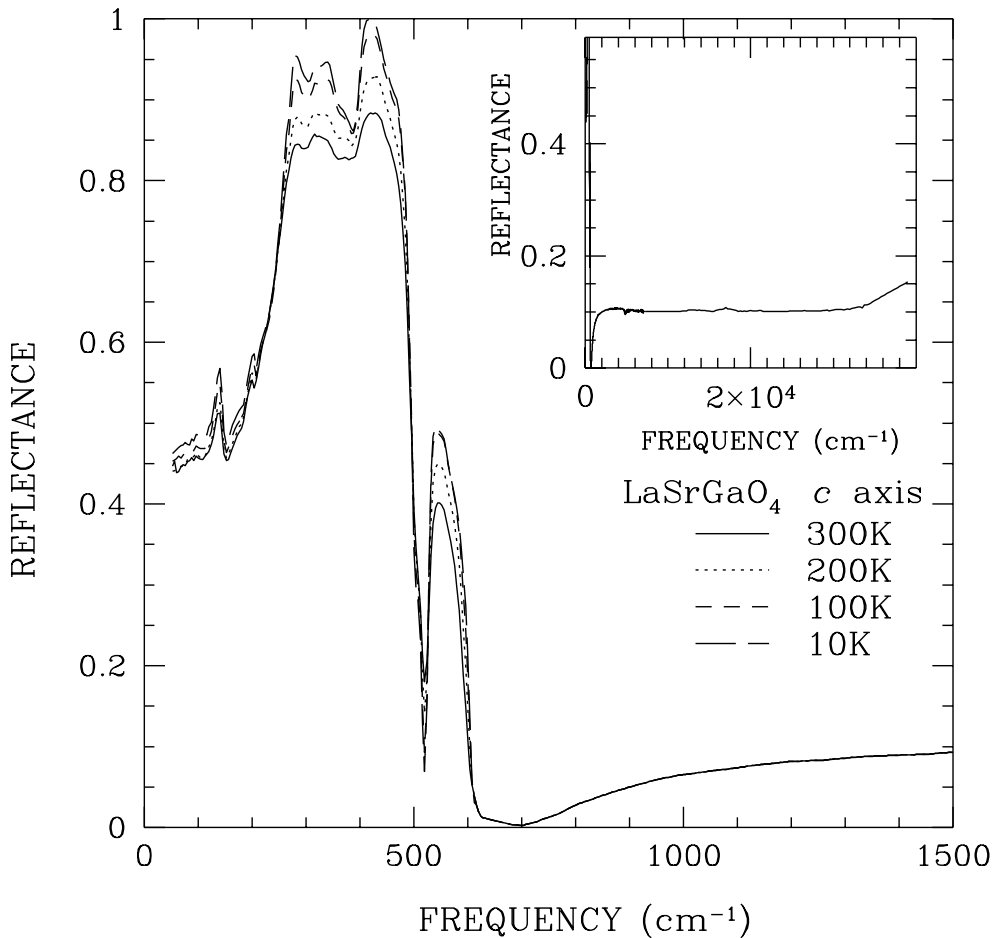


Fig. 2. Temperature dependence of the  $c$  axis reflectance of  $\text{LaSrGaO}_4$  from  $50 \text{ cm}^{-1}$  to  $1000 \text{ cm}^{-1}$  at 300K (solid lines), 200K (dotted line), 100K (short dashed line), and 10K (long dashed line). The inset shows reflectance spectrum for 300K out to  $40000 \text{ cm}^{-1}$ .

where  $\epsilon_1 = (n^2 - k^2)$  and  $\sigma_1 = 2nk\omega/4\pi$ .

Figure 3 and Figure 4 show the temperature dependence of the real part of the dielectric function and the conductivity for the  $a$  axis and  $c$  axis polarizations respectively. Due to the significant spectral weight at frequencies above  $40000 \text{ cm}^{-1}$ , the calculation of these properties is dependent on the choice of high-frequency extrapolation. As a result the curves have only been presented up to  $1000 \text{ cm}^{-1}$  as below this frequency there was only a weak dependence on the high-frequency extrapolation. An  $\omega^{1/2}$  extrapolation out to  $5 \times 10^5 \text{ cm}^{-1}$  followed by an  $\omega^{-4}$  form above this frequency were used to perform the Kramers-Kronig calculation.[20] A quadratic extrapolation to  $R_0$  as  $\omega \rightarrow 0$  was used for the low frequencies. Looking at Figure 3 (b), the phonon peaks in the conductivity all increase with decreasing temperature with little

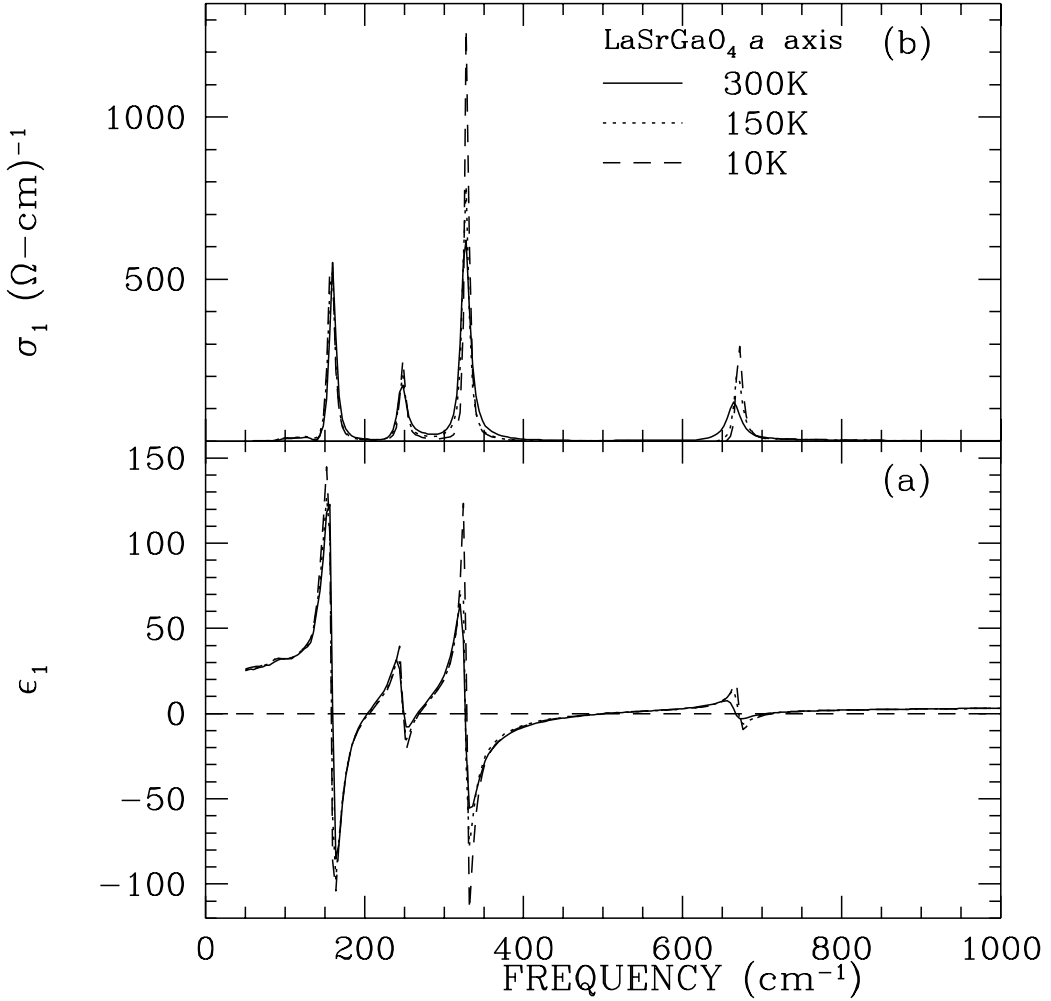


Fig. 3. Temperature dependence of *a* axis dielectric (a) and conductivity (b) of LaSrGaO<sub>4</sub>. The temperatures shown are 300K (solid line), 150K (dotted line), and 10K (dashed line).

shift in position, except for the peak at about 675 cm<sup>-1</sup> which can be seen to harden with decreasing temperature. None of the *c* axis phonon peaks in Figure 4 (b) shift significantly.

In addition to performing the Kramers-Kronig calculation, the reflectance data was fitted to a factorized form of the dielectric function [21] using a non-linear least-squares technique. The form of the dielectric is as follows:

$$\tilde{\epsilon}(\omega) = \epsilon_{\infty} \prod_j \frac{\omega_{LO,j}^2 - \omega^2 - i\omega\gamma_{LO,j}}{\omega_{TO,j}^2 - \omega^2 - i\omega\gamma_{TO,j}}, \quad (4)$$

where  $\omega_{LO,j}$ ,  $\omega_{TO,j}$ ,  $\gamma_{LO,j}$ , and  $\gamma_{TO,j}$  are the frequencies and widths of the *j*th LO and TO modes, respectively.

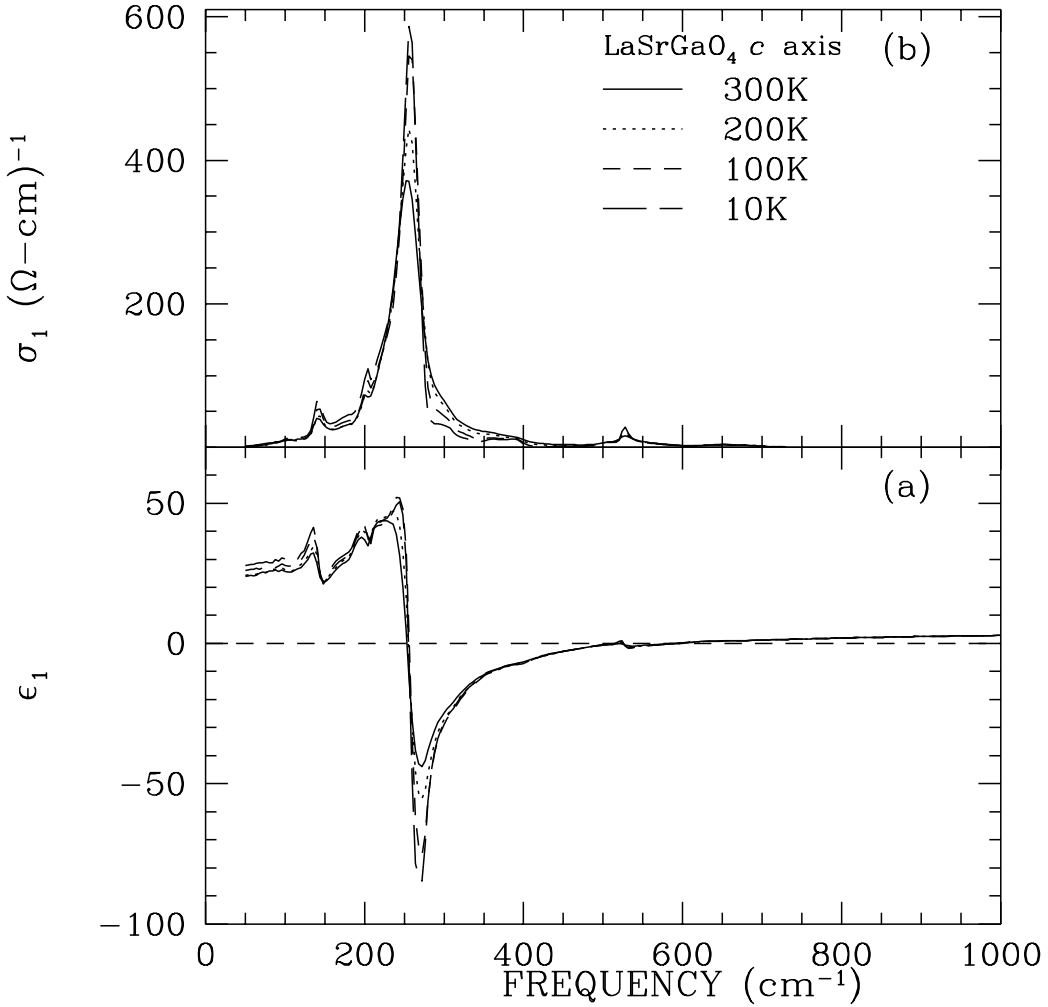


Fig. 4. Temperature dependence of *c* axis dielectric (a) and conductivity (b) of LaSrGaO<sub>4</sub>. The temperatures shown are 300K (solid line), 200K (dotted line), 100K (short dashed line), and 10K (long dashed line).

The results of the fits are summarized in Tables 1 and 2 for the *a* and *c* axis data, respectively. The fitting parameters have been limited by setting  $\gamma_{LO,j}$ , and  $\gamma_{TO,j}$  equal. The oscillator strength for each mode,  $\omega_{pi}^2$  can be calculated using[22]:

$$\omega_{pi}^2 = \epsilon_\infty(\omega_{LO,i}^2 - \omega_{TO,i}^2) \prod_{i \neq j} \frac{(\omega_{LO,j}^2 - \omega_{TO,i}^2)}{(\omega_{TO,j}^2 - \omega_{TO,i}^2)}, \quad (\gamma_{LO,i} = \gamma_{TO,i}). \quad (5)$$

and the  $\omega_{pi}$ 's calculated are listed in Tables 1 and 2.

The number of phonons used to fit the reflectance exceeds the number allowed by group theoretical considerations. However, the statistical nature of the La and Sr placement in the unit cells could result in additional IR-active phonons due to the broken symmetry. In particular, the lowest phonon peak in the ab

Table 1

Fitting parameters for the  $a$  axis reflectance data utilizing the factorized product form. All parameters are in  $\text{cm}^{-1}$  except for  $\epsilon_\infty$

Oscillator	300K	150K	10K
$\omega_{TO,1}$	104.97	103.64	101.31
$\omega_{LO,1}$	106.37	105.77	103.62
$\gamma_{LO,1}$	20.45	26.57	29.64
$\omega_{p1}$	98.22	120.55	124.73
$\omega_{TO,2}$	160.84	159.50	159.04
$\omega_{LO,2}$	203.34	205.14	205.94
$\gamma_{LO,2}$	6.51	5.45	4.83
$\omega_{p2}$	540.49	543.65	551.26
$\omega_{TO,3}$	246.73	247.17	247.80
$\omega_{LO,3}$	269.09	269.33	269.10
$\gamma_{LO,3}$	15.20	10.89	8.01
$\omega_{p3}$	372.99	355.28	348.26
$\omega_{TO,4}$	327.43	327.99	328.91
$\omega_{LO,4}$	502.38	501.53	501.14
$\gamma_{LO,4}$	10.41	6.96	5.55
$\omega_{p4}$	687.11	668.27	676.89
$\omega_{TO,5}$	663.16	667.49	669.77
$\omega_{LO,5}$	707.60	710.03	712.00
$\gamma_{LO,5}$	21.67	13.65	10.35
$\omega_{p5}$	381.00	372.00	377.88
$\epsilon_\infty$	4.534	4.420	4.531

plane fitting is only included to account for a small shoulder in the reflectance data at approximately  $100 \text{ cm}^{-1}$ . The remaining 4 phonons result in a good fit to the reflectance spectrum excluding this shoulder. The  $c$  axis reflectance, due to its asymmetric peaks, requires 5 oscillators to provide a satisfactory fit to the reflectance. Figure 5 shows the reflectance for the room temperature data, both  $a$  and  $c$  polarizations, and the fits to the reflectance.

Some mode assignments can be tentatively applied to the fitted oscillators by comparison to mode assignments for other isomorphic crystals.[2,3] For the  $a$  axis polarization there is one more oscillator than is allowed by group

Table 2

Fitting parameters for the  $c$  axis reflectance data utilizing the factorized product form. All parameters are in  $\text{cm}^{-1}$  except for  $\epsilon_\infty$ .

Oscillator	300K	200K	100K	10K
$\omega_{TO,1}$	143.14	144.04	144.24	144.43
$\omega_{LO,1}$	147.00	149.00	150.33	149.33
$\gamma_{LO,1}$	15.25	22.55	18.22	13.22
$\omega_{p1}$	177.06	203.66	227.56	207.74
$\omega_{TO,2}$	203.00	203.08	202.46	201.31
$\omega_{LO,2}$	204.18	204.65	204.65	204.65
$\gamma_{LO,2}$	12.00	12.54	15.00	17.00
$\omega_{p2}$	147.90	168.20	194.94	243.25
$\omega_{TO,3}$	254.16	255.65	256.39	255.25
$\omega_{LO,3}$	398.57	395.57	397.00	394.00
$\gamma_{LO,3}$	36.22	29.73	23.65	20.88
$\omega_{p3}$	988.81	993.12	987.34	982.18
$\omega_{TO,4}$	399.33	396.35	397.34	394.61
$\omega_{LO,4}$	505.38	504.45	502.96	501.61
$\gamma_{LO,4}$	29.96	24.39	19.10	17.11
$\omega_{p4}$	63.32	66.10	43.39	58.80
$\omega_{TO,5}$	526.19	525.18	524.13	523.71
$\omega_{LO,5}$	593.24	595.77	597.39	599.08
$\gamma_{LO,5}$	41.87	36.74	32.82	32.65
$\omega_{p5}$	173.94	180.02	185.27	191.95
$\epsilon_\infty$	4.02	4.05	4.05	4.05

theory. However  $\omega_{TO,1}$  is a very weak mode and can be assumed to have been introduced by some symmetry breaking mechanism. Of the remaining oscillators,  $\omega_{TO,2}$  can be assigned to a mode where the La/Sr atoms move in opposition to the  $\text{GaO}_6$  octahedra since the larger mass of the La/Sr would result in a lower frequency of vibration. The remaining  $3\text{E}_u$  oscillators are vibrations internal to the  $\text{GaO}_6$  octahedra.[3]

The  $c$  axis polarization has two additional modes above what is allowed by group theory. The  $\omega_{TO,4}$  mode is very weak and of the remaining four oscillators, it is not obvious which one is not an  $A_{2u}$  mode. It may be that the

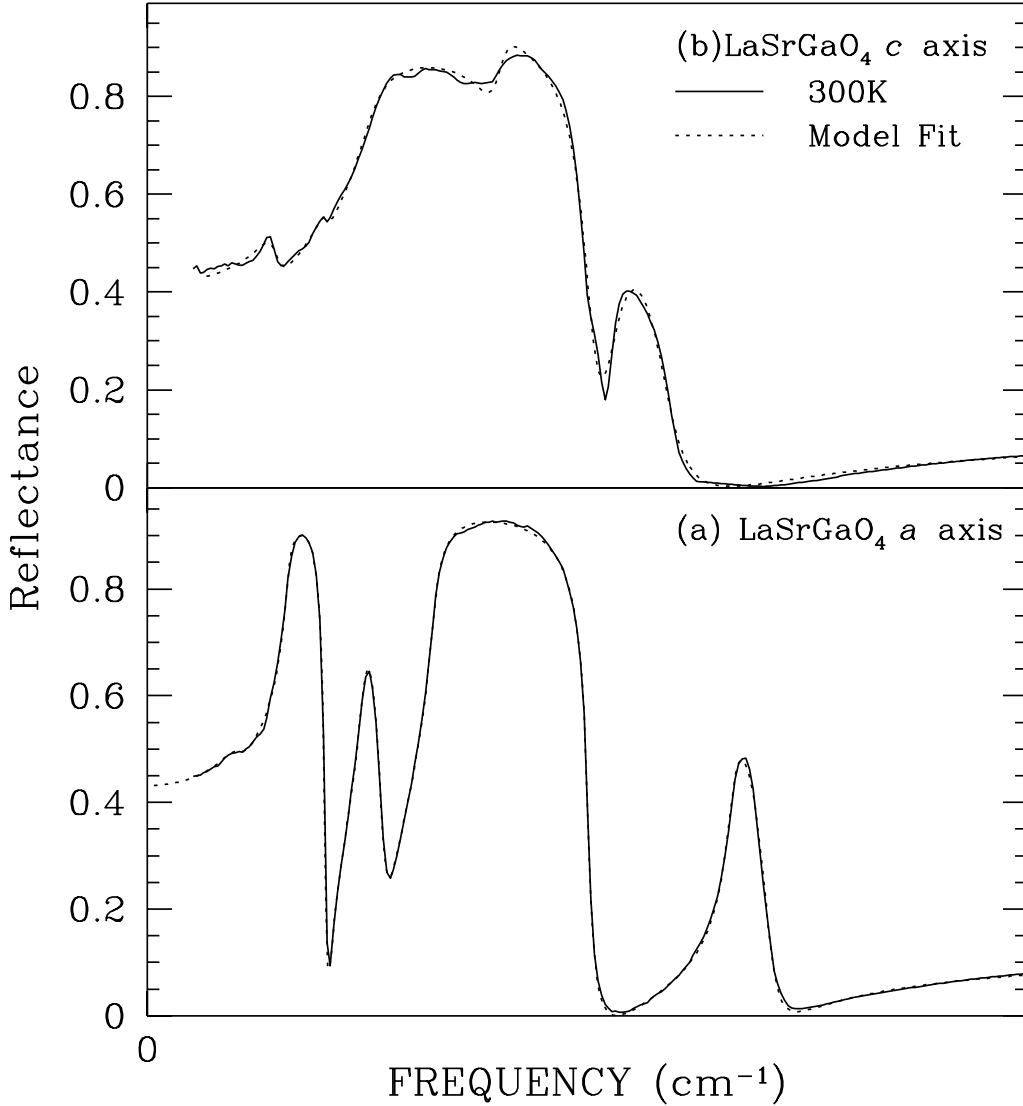


Fig. 5. Fits to room temperature reflectance of  $\text{LaSrGaO}_4$   $a$  and  $c$  axis polarizations. The solid lines are the reflectance data for 300K and the dotted lines are the fits calculated using values from Table I and II.

normally silent  $B_{2u}$  mode has been activated. The  $\omega_{TO,1}$  is likely the mode involving movement of the La/Sr atoms with respect to the  $\text{GaO}_6$  as it has the lowest frequency vibration. Similarly the highest two of the remaining strong modes,  $\omega_{TO,3}$  and  $\omega_{TO,5}$  are likely the  $A_{2u}$  modes since they involve vibrations of the light oxygen atoms. This leaves  $\omega_{TO,2}$  unassigned.

In conclusion, we have measured the reflectance of the single crystal,  $\text{LaSrGaO}_4$ , from 50 to 40000  $\text{cm}^{-1}$  for the  $a$  and  $c$  axes including temperature dependence from 300 K to 10 K. The optical properties are calculated using Kramers-Kronig transformations on the spectra and the temperature dependence of the real dielectric and conductivity has been presented. This allows the de-

pendence of the film spectrum on the substrate to be determined. This is of importance if the  $c$  axis reflectance is to be measured on  $\text{YBa}_2\text{Cu}_3\text{O}_{7-\delta}$  thin films or other High- $T_c$  materials grown on this substrate.

## Acknowledgements

The authors would like to thank C.C. Homes for useful discussions and aid in calculations. This work was supported by the Ontario Center for Materials Research (OCMR) and the National Science and Engineering Research Council (NSERC). A. McConnell would like to gratefully acknowledge the support of B. Clayman and the Department of Physics, Simon Fraser University.

## References

- [1] I. Rüter and Hk. Müller-Buschbaum, *Z. anorg. allg. Chem.*, **584**, 119-124 (1990).
- [2] G. Burns, F.H. Dacol, G. Kliche, W. König, and M.W. Shafer, *Phys. Rev. B* **37** (7), 3381-3388 (1988).
- [3] S. Tajima, T. Ido, S. Ishibashi, T. Itoh, H. Eisaki, Y. Mizuo, T. Arima, H. Takagi, and S. Uchida, *Phys. Rev. B* **43** (13), 10496-10507 (1991).
- [4] K. Nakamura, R. Katuno, and I. Aoyama, *Phase Transitions* **42**, 99-102 (1993).
- [5] S. Hontsu, J. Ishii, T. Kawai, and S. Kawai, *Applied Phys. Lett.* **bf 59** (22), 2886-2888 (1991).
- [6] A.W. McConnell, R.A. Hughes, A. Dabkowski, H.A. Dabkowska, J.S. Preston, J.E. Greedan, and T. Timusk, *Physica C* **225**, 7-12 (1994).
- [7] W. Ito, Y. Yoshida, S. Mahajan, and T. Morishita, *Physica C*, **227**, 313-320 (1994).
- [8] S. Hontsu, N. Mukai, J. Ishii, T. Kawai, and S. Kawai, *Applied Phys. Lett.* **61** (9), 1134-1136 (1992).
- [9] Y. Suzuki, D. Lew, A.F. Marshall, M.R. Beasley, and T.H. Geballe, *Phys. Rev. B* **48**, 10642-10645 (1993).
- [10] M. Mukaida and S. Miyazawa, *Applied Phys. Lett.* **63** (6), 999-1001 (1993).
- [11] T. Ishibashi, T. Fujita, Y. Okada, and M. Kawabe, *Jpn. J. Appl. Phys.* **32** Pt. 2 No.2B, L257-L259 (1993).
- [12] Z. Wen, I. Iguchi, and K. Nakamura, *J. Appl. Phys.* **69** (10), 7363-7265 (1991).

- [13] D.J. Lew, Y. Suzuki, A.F. Marshall, T.H. Geballe, and M.R. Beasley, Applied Phys. Lett. **65** (12), 1584-1586, (1994).
- [14] T. Matsui, T. Suzuki, H. Kimura, K. Tsuda, M. Nagano, and K. Mukae, Jpn. J. Appl. Phys., **31** Pt.2 No.6B, L780-783 (1992).
- [15] S. Hontsu, N. Mukai, J. Ishii, T. Kawai, and S. Kawai, Applied Phys. Lett. **64** (6), 779-781 (1994).
- [16] T. Konaka, M. Sato, H. Asano, and S. Kubo, J. Superconductivity, **4** (4), 283-288, (1991).
- [17] J. Petzelt and N. Setter, Ferroelectrics, **150**, 89, (1993).
- [18] A. Dabkowski, H.A. Dabkowska, and J.E. Greedan, J. Cryst. Growth, **132**, 205-208 (1993).
- [19] C.C. Homes, M. Reedyk, D.A. Crandles, and T. Timusk, Applied Optics **32**, 2976 (1993).
- [20] F.W. Wooten, *Optical Properties of Solids*, (Academic Press, New York, 1972).
- [21] A.S. Barker, Jr., in *Far-Infrared Properties of Solids*, edited by S.S. Mitra and S. Nudelman (Plenum, New York, 1970), p. 247.
- [22] L. Genzel, T.P. Martin, and C.H. Perry, Phys. Stat. Sol. (b) **62**, 83 (1974).